Date of publication xxxx 00, 0000, date of current version xxxx 00, 0000.

Digital Object Identifier 10.1109/ACCESS.2017.Doi Number

The Effect of the Ring Mains Units for On-line Partial Discharge Location with Time Reversal in Medium Voltage Networks

A. Ragusa[1], Member, IEEE, P. A. A. F. Wouters[2], H. Sasse[1] and A. Duffy[1], Fellow, IEEE

[1] School of Engineering and Sustainable Development, De Montfort University, Leicester LE1 9BH, UK.

[2] Department of Electrical Engineering, Eindhoven University of Technology, Eindhoven 5600 MB, The Netherlands

Corresponding author: A. Ragusa (e-mail: antonella.ragusa@dmu.ac.uk).

This work was supported by the European Union's Horizon 2020 Research and Innovation Programme under the Marie Skłodowska-Curie Grant under Agreement 838681.

ABSTRACT The performance of a new on-line partial discharge (PD) location method based on the Electromagnetic Time Reversal (EMTR) theory and the Transmission Line Matrix (TLM) method are investigated for characterization of Medium-Voltage (MV) networks. The generated distortion of the PD signal during its propagation along a network with realistically modelled components is reproduced in simulation and the effectiveness of the EMTR-based method to localise the PD source is analyzed. In particular, the effects of the ring main units (RMUs), that behave as a complex impedance, the variation with frequency of the MV cable impedance and the reflection patterns, due to impedance mismatches, are considered and investigated. Simulation results are given showing the performance of the EMTR method in two different networks configurations: the former one with a RMU at the end of a MV cable and the latter one with a second MV cable connected to the RMU of the first configuration having a distribution transformer at its far end. The results show that the EMTR method is able, with only a single observation point, to localise PDs also in the presence of RMU with a relative error, with respect to the line length, of approximately 1%.

INDEX TERMS Partial Discharge, On-line partial discharge location methods, Electromagnetic Time Reversal, Medium Voltage Networks, PD signal distortion.

I. INTRODUCTION

Partial discharge (PD) events, that are localized electrical discharges starting in discontinuities or defects of the insulation system [1], are often the cause of the power cables insulation degradation in power networks [2]. The failure of power cables' insulation in power networks leads to severe social and economic consequences producing effects ranging from faults to blackouts and supply interruption. Because statistic indicates that more than 85% of equipment faults are linked to insulation failure [3], PD is widely considered as one of the best 'early warning' indicators of cable failure [2] and, the adoption of on-line PD location is regarded as the most suitable method to monitor the network integrity and improve its resilience and reliability [2][3]. The on-line PD location methods is, indeed, a desired feature in the protection schemes of the modern power networks to prevent faults and guarantee the electricity security [2][4].

Currently, the on-line PD location is performed mostly using methods based on reflectometry or traveling wave techniques [5]-[10]. These techniques work on the fact that a PD event produces electromagnetic waves that travel towards the cable ends. Most of the used methods are based on multi-end measurements [5]-[7], simultaneously in two or more observation points (OPs) of the line, of the direct PD wave, coming directly from the PD source, and the reflected waves from the cable ends. The PD source is located evaluating the times of arrival of the measured signals (time of arrival, ToA, methods). But the need of synchronization makes their practical implementation difficult. Furthermore, the distortion of PD signal during its propagation along the line, due to impedance mismatches and variation of the cables and components impedances with the frequency, and the presence of electromagnetic interference (EMI) on power networks affect the accuracy of the reflectometry methods. Wavelet techniques (WTs) [8]-[11] are often used to solve some of the shortcomings of the reflectometry methods, but WTs require a huge amount of computational effort. A new method for the on-line PD location has been proposed [13]-[16] based on the

use of the EMTR (Electromagnetic Time Reversal) theory [12] and the Transmission Line Matrix (TLM) method to describe the EMTR propagation of the PD signals. EMTR theory has been adopted, recently, for the localization of electromagnetic disturbance sources on power systems [12][17][18], showing improved performances with respect to the traditional location techniques, due to the fact that it is possible to apply them in inhomogeneous and complex networks, they need only one observation point to localize the source and are robust against the presence of noise. In [13] the basic design of the new EMTR-based PD location method has been proposed. Its effectiveness to locate PDs using only one observation point has been theorical demonstrated for lines with homogeneous [13][16] and inhomogeneous [14][15][16] cable sections. In [14] its experimental validation is given, showing the its effectiveness to locate PDs in real Medium Voltage (MV) homogeneous power cables and its robustness against the presence of noise has been also analyzed and proved. The EMTR-based PD location method has also shown to allow a PD location with a good accuracy without too many requirements on the needed input parameters, requiring only the knowledge of the signal velocity and the cable lengths.

In this paper the effect of the ring main units (RMUs) on the effectiveness of the EMTR method in MV power grids is analysed in simulation. Power cables on MV grids terminate at ring main RMUs. A distribution transformer at the RMU together with the cable connecting the transformer to the busbar behaves as a complex impedance. This is a cause of distortion of the PD signal and, consequently, the signal transfer to the measurement sensor is imprecisely known. In addition, other outgoing MV cables may affect the reflection patterns further distorting the PD signal [19][20]. In this work the effect of these distortions on the performance of the EMTR PD location method are analysed in two different lines configurations. The paper is organised as follows. In Section II, the EMTR-based method is briefly introduced. Section III the distortion of the PD signal due to the grid components, complex impedance of cables and of RMUs, is described and the adopted models to reproduce it are detailed. In Section I the performance of the EMTR method are discussed in the two considered cline configurations.

II. TIME REVERSAL METHOD FOR PD LOCALISATION

The PD location method based on EMTR theory [13] is based on the invariance under time reversal of the Telegrapher's Equations for non-dissipative lines [12]. For non-dissipative lines, the telegrapher's equations are given by:

$$\frac{\partial v(x,\ t)}{\partial x} + L\frac{\partial i(x,t)}{\partial t} = 0 \qquad (1.\mathrm{a})$$

where L and C are the per unit length series inductance and shunt capacitance of the line. The propagation speed, u, and a characteristic impedance, Z_c, of the line are given by:

$$u = \frac{1}{\sqrt{LC}} \quad ; \quad Z_c = \sqrt{L/C} \qquad (2)$$

Applying the time-reversal transformation, equations (1) become:

$$\frac{\partial v(x,\ -t)}{\partial x} + L\frac{\partial(-i(x,-t))}{\partial(-t)} = 0 \qquad (3.\mathrm{a})$$

$$\frac{\partial(-i(x,\ -t))}{\partial x} + C\frac{\partial(v(x,-t))}{\partial(-t)} = 0 \qquad (3.\mathrm{b})$$

Equations (3) are identical to equations (1), except for that the current sign that has changed [12]. The invariance under time reversibility implies that the voltage and current, *v(x,t),* and *i(x,t)*, and their symmetric values in time, *v(x,-t),* and *i(x,-t),* are both solutions of the telegrapher's equations.

The invariance under time reversal of the propagation equations and the spatial correlation property of the time reversal theory allow the refocusing of the time reversed back-propagated PD signals into its original source.

The designed EMTR PD location method, uses the Transmission Line Matrix (TLM) numerical method [21] to solve the equations (3) describing the time reversal propagation of the PD signals. In particular, the EMTR simulations are performed using a 1D lossless TLM model of the system under study. The TLM method is a time-domain differential-equation-based method, that discretizes the transmission line, of length L, into a series of N segments, of length Δx, connected as shown in Fig. 1 (a). Each LC section is represented by a transmission line of impedance Z_c, given by relation (2), and characterized by a transit time Δt given by:

$$\Delta t = \frac{\Delta x}{u} = \Delta x \cdot \sqrt{LC} \qquad (4)$$

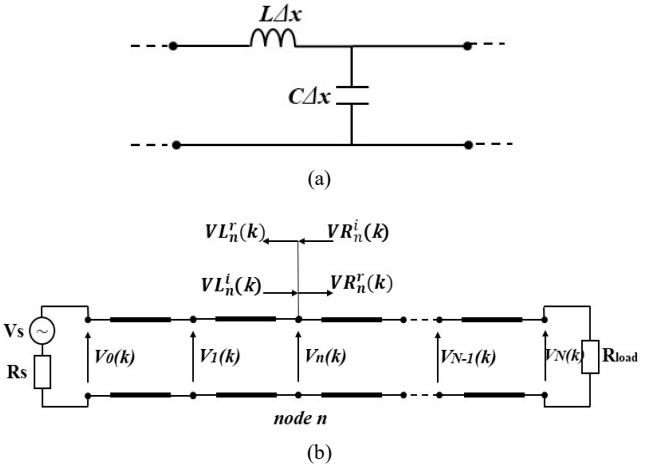

FIGURE 1 Equivalent circuit of a power line node (a), its TLM model (b), and the Thevenin equivalent circuit (c) at the node n.

Connecting the N sections, the TLM equivalent model of the line is obtained, as shown in Fig. 1 (b). At each node, the voltage pulses, $V_n(k)$, are scattered as they propagate in the lines, generating incident voltages, $VL^i{}_n(k)$ and $VR^i{}_n(k)$, and reflected voltages, $VL^r{}_n(k)$ and $VR^r{}_n(k)$, respectively on the left and on the right-hand side of the node. Replacing the lines to the right and to the left of the node n by their Thevenin equivalent circuits, and applying Millman's theorem, the voltage $V_n(k)$, and the current $I_n(k)$, at time step k, are evaluated for each node of the network [21].

The basic steps of the EMTR method to locate PDs [13]-[16] are shown in Fig. 2 and are the following:

1. Measurement of the PD signal, $s(x,t)$, at one observation point (OP) along the network.
2. Time reversal the measured PD signal.
3. Definition of guessed PD locations (GPDLs) in nodes of the 1D TLM model of the network.
4. Simulation of the back-injection of the time-reversed PD signal for different GPDLs.
5. Location of the PD source by finding the GPDL characterized by the maximum energy.

The GPDL node reproduces the line transversal capacitance in the cable insulator modified by the PD event [13]. For each TR simulation the energy, E_n, stored in the transversal impedance of the GPDL is evaluated, normalized with respect to the maximum energy as follows:

$$En = \frac{\frac{1}{2}C\sum_{k=1}^{M} V_{GPDL}^2(k)}{\frac{1}{2}C\sum_{k=1}^{M} V_{GPDL\_m}^2(k)} \quad with \quad M = T/\Delta t \qquad (5)$$

where $V_{GPDL\_m}(k)$ is the maximum voltage over all the GPDLs and M the number of the samples.

When the method is used in practice, the first step of the procedure, is carried out experimentally [14]. In this work, the first step is substituted by a direct time (DT) simulation, using a lossy model of the system under study that is able to reproduce the PD signal distortion during propagation in real grids, as described in the Section III.

III. SIGNAL DISTORTION BY GRID COMPONENTS

In the following subsections, the models of each component of the grid that affects the PD signal propagation, distorting the signal, are described. Then, the related reflection patterns are also analysed.

A. CABLE MODEL

The propagation coefficient of an XLPE cable is modelled by numerically evaluating the harmonic cable impedance $Z(\omega)$ and admittance $Y(\omega)$ with electromagnetic simulation software (Oersted and Electro from IES [22]). The applied cable geometry and material properties are provided in Table I. The characteristic impedance Z_c and the propagation coefficient γ are obtained from:

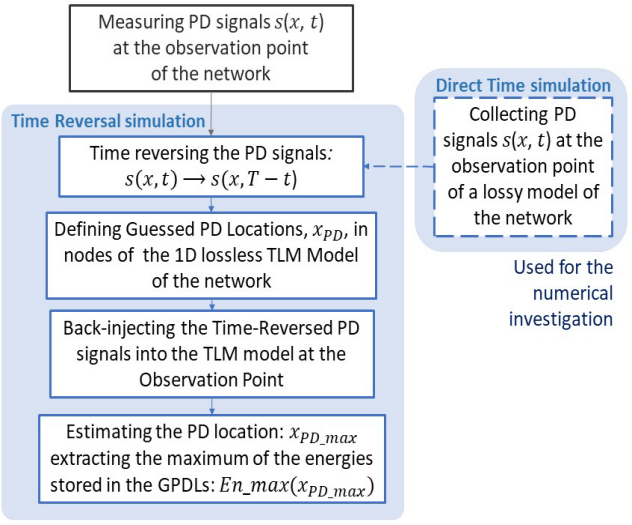

FIGURE 2. EMTR-based method for the on-line localization of PDs [15].

$$Z_c = \sqrt{\frac{Z}{Y}} \quad \text{and} \quad \gamma = \alpha + \mathrm{j}\beta = \sqrt{ZY} \qquad (6)$$

The characteristic impedance, the phase velocity $u=\omega/\beta$ and the per-unit-length attenuation α are shown in Fig. 3. The curves are smooth and therefore simulation for only a limited number of frequencies (1-2-5 sequence from 1 kHz to 100 MHz) suffices. The curves are linearly resampled with 1 kHz steps to allow for calculation of the time-domain responses via the inverse Fourier transform.

The characteristic impedance is close to constant for the relevant frequency range for signal propagation in power cables. A constant real value of 13.6 Ω was used. The propagation velocity amounts to about 163 m/µs. The attenuation arises from the conductor losses and losses from the semi-conductive (s.c.) layers. The latter becomes dominant as from about 8 MHz.

The reflection pattern from a pulse starting from one side in a single cable segment can be modelled by the transfer function:

$$H(\omega) = \frac{\tau_{obs}(\omega)\rho_1(\omega)\mathrm{e}^{-2\gamma_1(\omega)L_1}}{1-\rho_1(\omega)\rho_{obs}(\omega)\mathrm{e}^{-2\gamma_1(\omega)L_1}} \qquad (7)$$

TABLE I
DESIGN AND MATERIAL PARAMETERS OF THE MODELLED XLPE CABLE

Cable parameter	Value
outer jacket radius	19.0 mm
earth screen radius	16.6 mm
insulation screen radius	15.6 mm
XLPE insulation radius	14.5 mm
conductor screen radius	11.0 mm
conductor radius	10.3 mm
resistivity of conductor (Al)	$3.69{\cdot}10^7$ S/m
resistivity of earth screen (Cu)	$5.84{\cdot}10^7$ S/m
relative permittivity of XLPE	2.23-0.001j
relative permittivity s.c. screens	1000
conductivity of s.c. screens	33 S/m

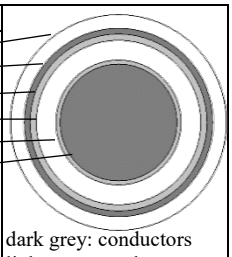

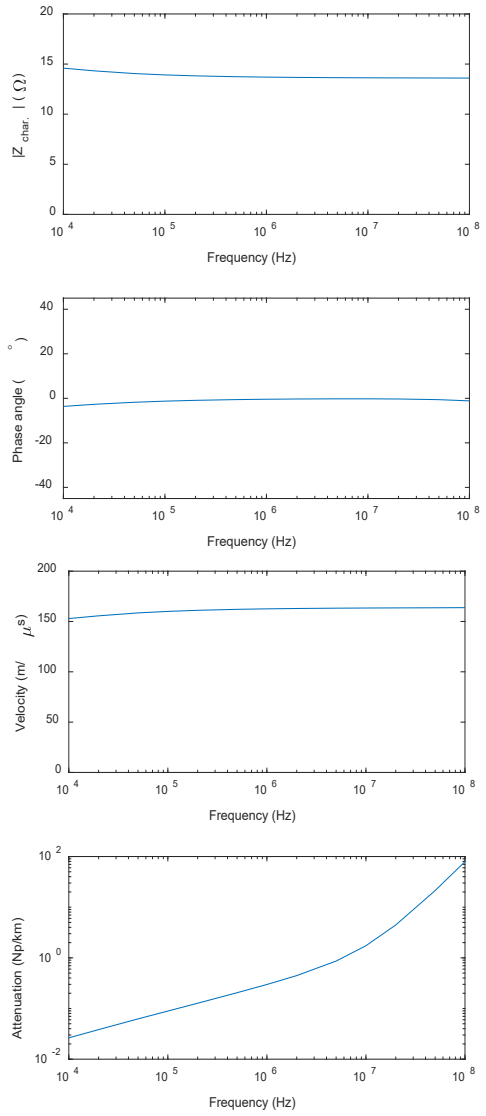

FIGURE 3: Simulated cable characteristic impedance, phase velocity and attenuation

The numerator accounts for the signal propagation up and down the cable with length L_1, the reflection coefficient $\rho_1(\omega)$ at the far end and the transmission coefficient $\tau_{obs}(\omega)$ from the detection impedance at the observation point. The denominator accounts for multiple reflections, which involves, besides $\rho_1(\omega)$, the reflection coefficient $\rho_{obs}(\omega)$ at the observation point. It will be assumed that the initial pulse is narrow, meaning that after travelling some distance along the cable its waveform is fully determined by the cable propagation coefficient $\gamma_1(\omega)$. Then, the initial pulse can be approximated as a Dirac pulse and the transfer function $H(\omega)$ directly represents the reflection pattern in the frequency domain.

The reflection pattern depends on the transition between the cable characteristic impedance Z_{c1} and the impedance seen at the far end. This can, e.g., be a lumped impedance or the input impedance Z_{in} of a connected cable (length L_2, propagation coefficient $\gamma_2(\omega)$ and characteristic impedance Z_{c2}):

$$Z_{in}(\omega) = Z_{c2}\frac{1+\rho_2(\omega)\mathrm{e}^{-2\gamma_2(\omega)L_2}}{1-\rho_2(\omega)\mathrm{e}^{-2\gamma_2(\omega)L_2}} \tag{8}$$

The reflection coefficient $\rho_2(\omega)$ depends on the load at the end of the second cable. Further cable cascading can be accomplished by substituting the reflection coefficient at the next cable segment here.

B. RMU MODEL

Small RMUs are usually only a few meters in size containing one or a few medium-voltage cables connected to a busbar and a distribution transformer that feeds a local low-voltage grid. A lumped component model is proposed in [19] aiming to describe the influence of an RMU on partial discharge propagation, see Fig. 4. The values of the model parameters were determined by injecting a pulse at the far end of one of the cables and measuring the responses at several locations inside the RMU [20]. The RMU is subdivided in compartments, each containing a single network component. The cables in compartments 1 and 2 are each modelled with its characteristic impedance and inductances related to loops from the connection to the busbar:

- Z_c: The characteristic impedance determined by the cable model;
- L_c: The contribution to the loop inductance from the connection to the busbar;
- L_{bb}: The contribution to the loop inductance from the busbar.

Compartment 3, which contains the distribution transformer, includes:

- C_{tr}, L_{tr}, R_{tr}: The transformer behaves mainly capacitively for the main frequency components present in partial discharge signals. It is modelled as a capacitance in series with the inductance and resistance.
- C_{tcc}, L_{tcc}, R_{tcc}: The transformer is connected to the busbar through power cables. These cables provide a capacitive load and are modelled together with inductance and resistance.
- The connection to the busbar is modelled with L_c and L_{bb}.

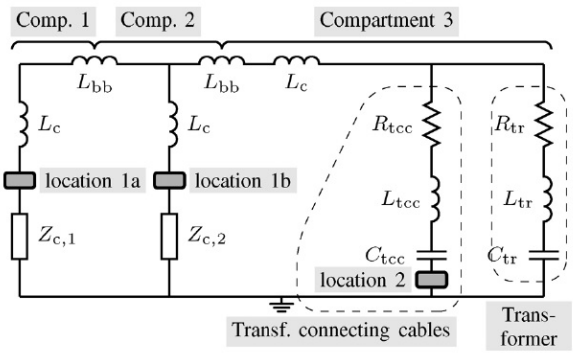

FIGURE 4 RMU compartment model [19].

TABLE II
FITTED PARAMETERS USED FOR MODELLING THE HIGH-FREQUENCY BEHAVIOUR OF AN RMU [19]

Z_c (Ω) [1]	L_c (µH)	L_{bb} (µH)	C_{tr} (nF)	L_{tr} (µH)	R_{tr} (Ω)	C_{tcc} (nF) [2]	L_{tcc} (µH)	R_{tcc} (Ω)
13.6	0.34	0.12	2.5	2.6	12	1.9	1.2	8.6

1) Characteristic impedance Z_c is obtained from electromagnetic modelling the cable design
2) Capacitance C_{tcc} is determined from the cable length and its specifications

Table II provides the parameters for the modelled RMU, which are taken from [19]. They are an average of the values obtained from tests at six RMUs. These parameters are based on best fitting over a frequency range from 200 kHz up to 5 MHz. This frequency range is most relevant for signal propagation along medium-voltage cables ranging from hundreds of metres up to several kilometres.

From this model, the impedance of the load at a cable end can be determined. Considering the cable in compartment 1 as the cable to be diagnosed, it is loaded via the impedance from L_c and L_{bb} to the branches that represent the cable in compartment 2 and the parallel branches of the transformer and its connection in compartment 3. When the RMU is situated at the end of a medium-voltage connection, it is only loaded with the transformer and the contribution of the cable in compartment 2 can be removed.

The impedance as seen from the diagnosed cable is shown for both cases in Fig. 5. The inductances, related to the loops formed by the busbar connection, together with the capacitances from the transformer and connecting cables cause resonances in the low megahertz range. These resonances distort the signal waveforms from partial discharge signals as they occur at relevant frequencies for signal propagation along power cables. At lower frequencies either the capacitances dominate the impedance (blue curve) or the characteristic impedance of the second cable (red curve). Beyond the resonances, the substation impedance increases due to the inductances.

Modelling of the reflection pattern from an RMU at the cable termination is accomplished by using the RMU impedance in the calculation of the far end reflection coefficient. When there is a second cable connected that also adds reflections from its far end, it can be modelled using its input impedance Z_{in} rather than its characteristic impedance Z_{c2} in the scheme of Fig. 4. The parameters in the RMU model were determined accounting for frequencies up to about 5 MHz [20]. For higher frequencies, connection details become important, which are specific for each RMU. In practice for power cable diagnostics, these frequencies hardly contribute due to signal attenuation and the generic model of Fig. 4 provides a representative picture of the influence of RMUs on partial discharge waveforms.

C. REFLECTION PATTERNS

The signal distortion by an RMU can be illustrated by injecting a signal at one end of the cable and simulating its reflections when the cable is terminated by an RMU. For illustration purposes, the near end is terminated with a real valued detection impedance making τ_{obs} and ρ_{obs} real as well. The applied initial signal is a Dirac pulse and the detection is bandwidth limited (50 kHz – 5 MHz). For the two cases, shown in Fig. 6, the reflections due to the RMU impedance are depicted in Fig. 7. The two cases are described in the following:

- CASE 1: The cable length is 1000 m and the RMU only consists of the distribution transformer (blue curve). The pattern shows periodic recurring reflections. The inset shows the peak distortion by the complex RMU impedance. For later reflections, the cable propagation characteristics quench the higher frequencies. For the remaining frequency range, the impedance is high and the far end reflection coefficient approaches one. This results in less distorted peaks, which broaden and attenuate further because of the cable characteristics.
- CASE 2: A second cable is connected to the RMU at the far end with 800 m length having a distribution transformer at its far end (red curve). Cables and distribution transformers are modelled with the parameters in Tables I and II. The first reflection at the RMU is only easily observable for the first reflection. Multiple reflections disappear since for the relatively low remaining frequencies the impedance from the second cable dominates, which closely terminates the first cable characteristically. The far end reflections from the second cable remain contributing since this cable is connected to a transformer only, which behaves like an open circuit for low frequencies.

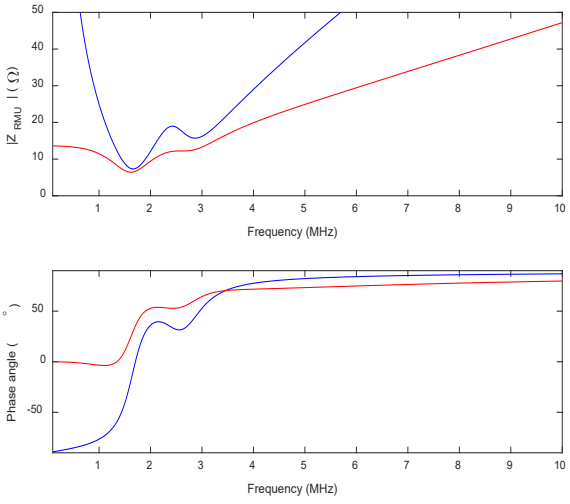

FIGURE 5: Impedance of an RMU with only a distribution transformer (blue) and including a second connected cable (red)

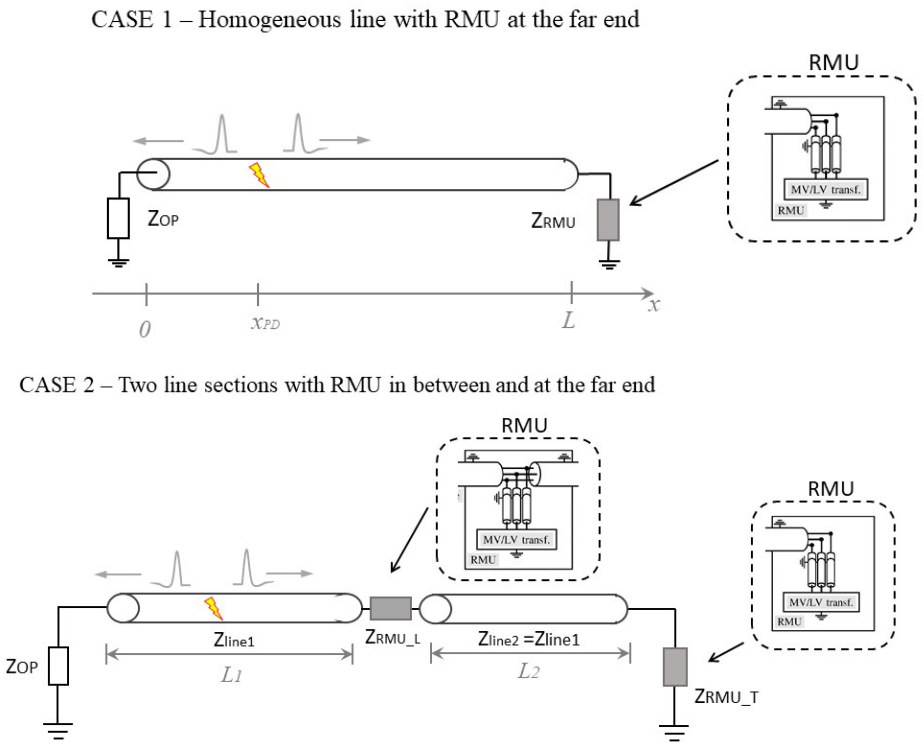

FIGURE 6: **Schematic of the two cases under analysis.**

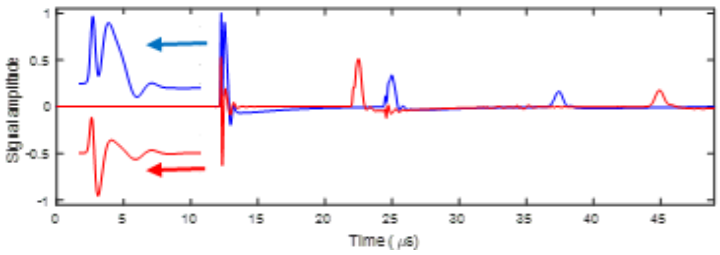

FIGURE 7: **Reflection pattern from 1000 m cable terminated with an RMU with only a distribution transformer (blue) and with, in addition, a cable with 800 m length (red); the insets show the first reflection peak over a 2 μs time scale**

Partial discharges which arise at some position X cause waves running in both directions. The total reflection pattern can be modelled from the sum of the contributing transfer functions:

$$H_X(\omega) = \tau_{obs}(\omega)\frac{e^{-\gamma_1(\omega)X} + \rho_1(\omega)e^{-\gamma_1(\omega)(2L_1-X)}}{1-\rho_1(\omega)\rho_{obs}(\omega)e^{-2\gamma_1(\omega)L_1}} \quad (9)$$

IV. TIME REVERSAL PD LOCATION FROM SIMULATION

A lossless 1D TLM model of the line has been developed for each case under analysis to perform the time reversal simulations for the PD localisation, as described in Section II. When PD signal propagates over distances of 1–2 km, most of the remaining energy is in the frequency range up to 1 MHz or few MHz [19], decreasing further for longer distances. Then, the PD signal, measured at the OP and used to perform the EMTR simulations, is characterised by a frequency content up to a few MHz. At these low frequencies, the inductances, and capacitances in RMU/substation can be neglected compared with the characteristic impedance of the cable Z_c, and the equivalent circuit of the RMU/substation can be approximated by the parallel connections of the characteristic impedances of the N-connected MV cables [19]. With this approximation, in the frequency range of interest, the input impedance of the RMU/substation, seen by the PD signal, Z_{RMU}, and the reflection coefficient at the RMU input, Γ_{RMU}, can be evaluated as follows [19]:

$$Z_{RMU} \approx \frac{Z_c}{N-1} \quad (9)$$

$$\Gamma_{RMU} = \frac{Z_{RMU}-Z_c}{Z_{RMU}+Z_c} \approx \frac{2-N}{N} \quad (10)$$

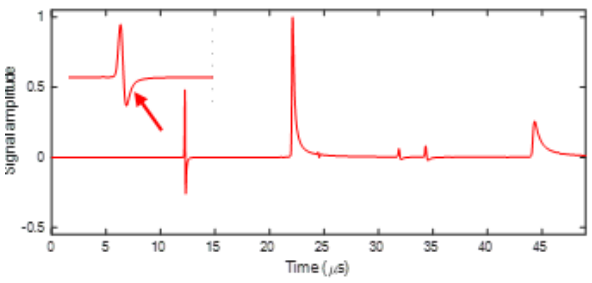

FIGURE 8: Reflection pattern from a 1000 m connected via a 3 m segment to an open ended 800 m cable; the inset show the first reflection peak over a 2 μs time scale

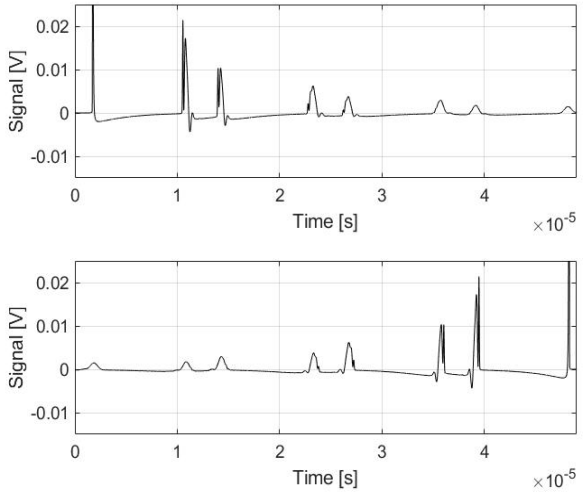

FIGURE 9: PD signal collected at the OP (upper) and the time reversed PD signal (lower) in CASE 1 when the PD source is at 280 m from the OP.

Hence, for the cases under analysis shown in Fig. 6, in the 1D TLM model the input impedance of the RMU at the line termination, Z_{RMU_T}, is $Z_{RMU\_T} >> Z_c$, then the reflection coefficient is equal to $\Gamma_{RMU\_T} = 1$. While when the RMU is in the middle of the line, it has been modelled with a TLM model 3m long with a characteristic impedance, Z_{RMU_L}, chosen equal to $Z_{RMU} = 2 \cdot Z_c$, so with a relative reflection coefficient equal to $\Gamma_{RMU\_L} = 0.5$. This is because, the RMU only causes a distortion mainly for high frequencies. It becomes invisible when the wavelengths associated with the remaining frequencies after signal attenuations are clearly exceeding the RMU size. A similar distortion occurs when modelling the RMU as a short transmission line (TL) with different characteristics. To illustrate this, two cables (1000 m and 800 m) are connected via a short cable length of 3 m with a characteristic impedance double that of the cable. The far end is kept open and a signal is injected at the observation point. As shown in Fig. 8, a somewhat less oscillatory response but still quite similar with decaying peaks as in Fig 7 (red curve) is obtained for the reflections at the short TL (at 12, 24, 32 and 34 μs), whereas the far end reflections (at 22 and 44 μs) remain clearly visible.

Finally, from the electromagnetic modelling of the cable, and considering the frequency range up to few MHz, for the design of the 1D TLM model the following characteristic impedance of the cable and propagation speed have been employed: $Z_c = 13.6\ \Omega$, $u = 1.625 \cdot 10^8$ m/s.

In each of the described cases, the PD signal has been collected at the observation point (OP) at the left end of the line. As explained in Section II, the collected PD signal is time reversed and injected into the 1D lossless TLM model of the system under study and several time reversal simulations are performed.

For the two analysed cases the following results have been obtained:

- CASE 1: Fig. 9 shows, for example, the collected PD signal at the OP and the time reversed signal when the PD source is 280 m from the OP. In Fig. 10-11 the simulation results, showing the performance of the of the EMTR-based PD location method are shown for cable lengths of respectively 1 km and 2 km. Table III summarizes the results for four PD positions (source) together with the located positions (EMTR).
- CASE 2: Fig. 12 shows the collected and time reversed PD signal when the PD source is at 300 m from the OP. The EMTR results are shown in Fig.13. The cable lengths are 1 km and 0.8 km. The accuracy of the localization is summarized in the last columns of Table III.

As the figures show the method is able to localize the PD source in each analysed case despite the distortion of the PD signal due to the frequency dependence of the systems impedances and the reflections at the impedance's mismatches.

The relative error in the localization, evaluated with respect to the line length, is generally below 1%, which is an acceptable error in practical applications. The error increases a little, but remains always lower than 1.5%, at the terminations in CASE 1 with the line length L=1 km.

To localise the PD source, a first scan of the system has been carried out choosing GPDLs 8 m apart from each other. After that, a refined search has been performed, reducing the distance between the GPDLs to 1 m only in the section of the line where the the maximum concentration of the energy associated to the time reversed signals propagation has been detected during the first scan.

A computational time of about 30 s is necessary for the line 1km long and of about 50 s for the line 2 km long, using a using a 64-bit pc with an Intel® Core™ i7-8700K, CPU at 3.70GHz, 32GB RAM and 1TB disk.

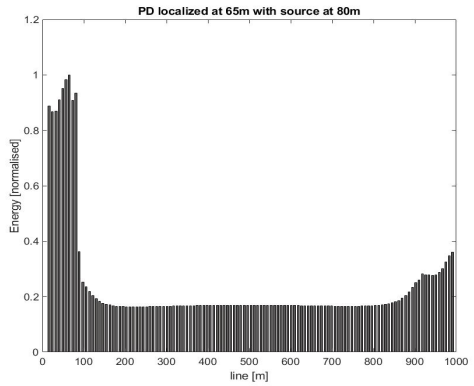

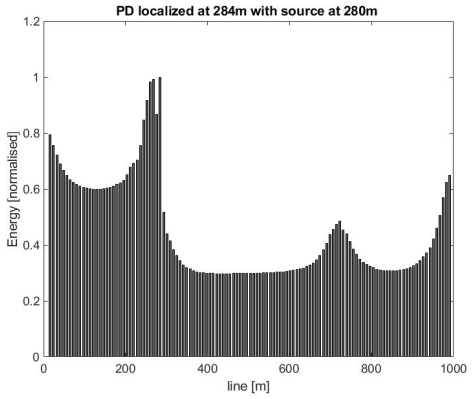

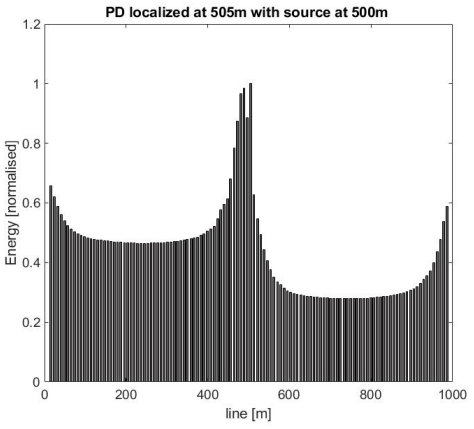

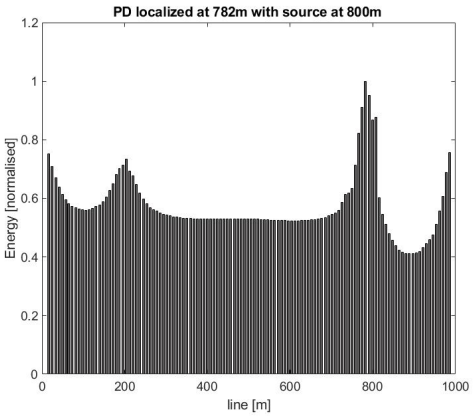

FIGURE 10: Simulation results of the EMTR-based PD location method in the CASE 1 with 1 km length of the line.

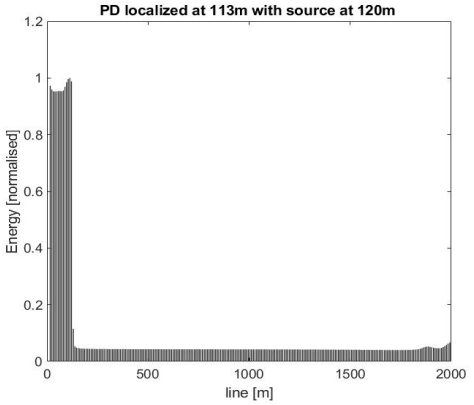

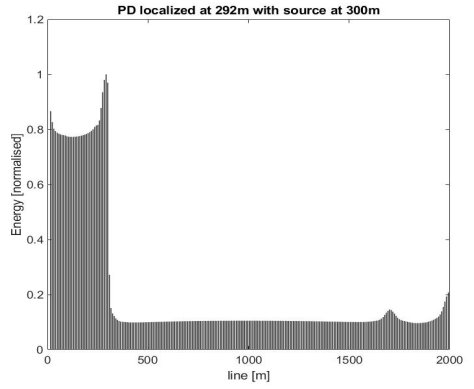

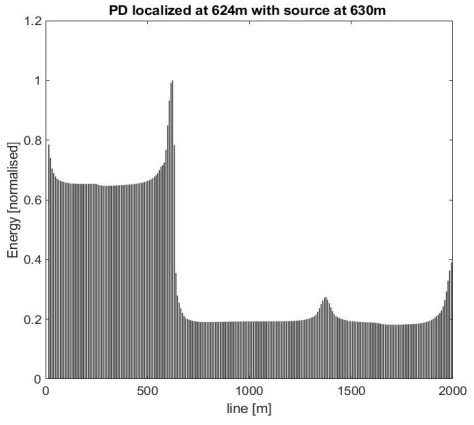

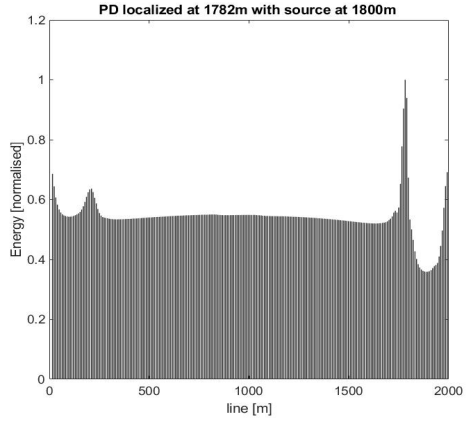

FIGURE 11: Simulation results of the EMTR-based PD location method in the CASE 1 with 2 km length of the line.

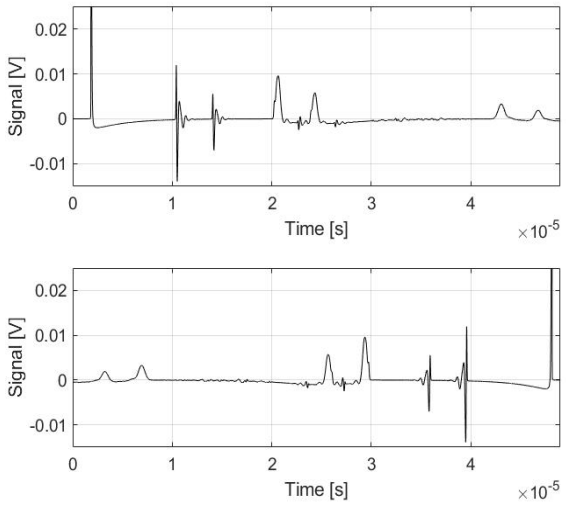

FIGURE 12: PD signal collected at the OP (upper) and the time reversed PD signal (lower) in CASE 2 when the PD source is at 300 m from the OP.

TABLE III
LOCALIZATION RESULTS OBTAINED WITH EMTR

CASE 1: 1 km		CASE 1: 2 km		CASE 2: 1 / 0.8 km	
Source	EMTR	Source	EMTR	Source	EMTR
80 m	65 m	120 m	113 m	300 m	281 m
280 m	284 m	300 m	292 m	700 m	683 m
500 m	505 m	630 m	624 m	1200 m	1183 m
800 m	782 m	1800 m	1782 m	1450 m	1434 m

VII. CONCLUSION

The performance of the EMTR-based method to locate PD with the presence of ring main units (RMUs) on the grid has been analysed in simulation. A description of the EMTR-based method is given and the models used to simulate the grids components, RMU and power cable, useful to reproduce the PD signal distortion are described. The effectiveness of the EMTR method to localize the PD source has been analyzed in two different configurations: 1). a homogeneous line, both 1 km and 2 km long, with one RMU at the far end and 2). Two cable section with an RMU in between and an RMU at the far end of the second cable section. The simulation results show that the EMTR method is able to localize PDs with a computational time less than a minute. For online monitoring, if this duration would be critical, the technique can be applied when pre-localization, e.g. by threshold discrimination, shows that certain PDs are concentrated or arise near a critical location. More accurate pinpointing of the defect can then be achieved with EMTR. The relative error, with respect to the total cable length, usually is below 1%, except when the PDs arise close to the cable terminations, where the error increases but never exceeded 1.5%.

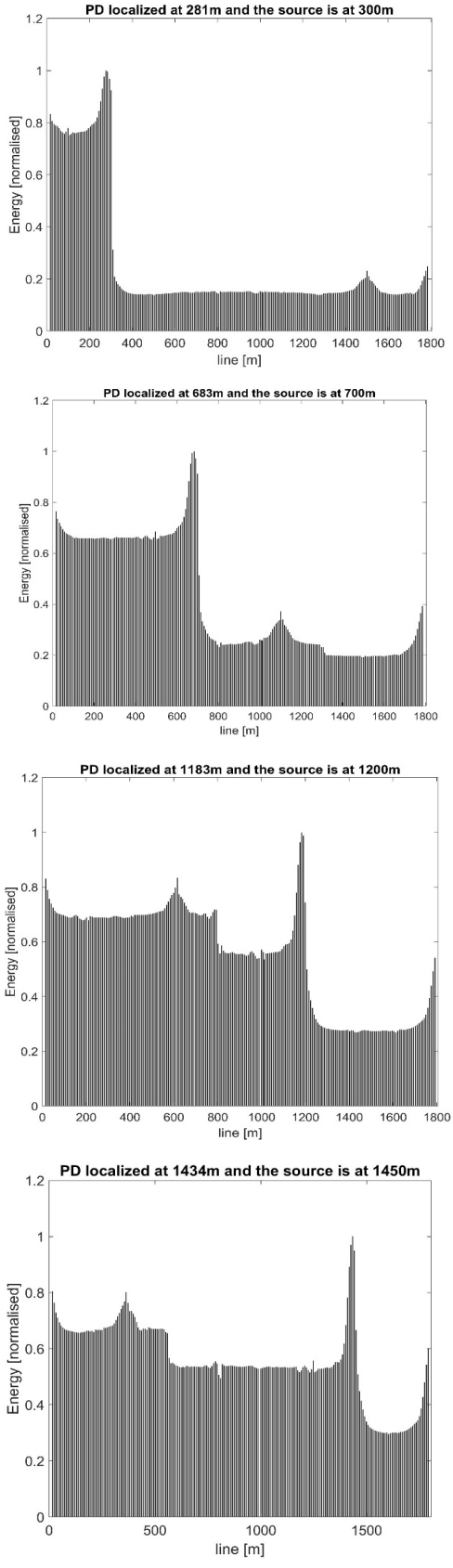

FIGURE 13: Simulation results of the EMTR-based PD location method in the CASE 2.

REFERENCES

[1] EN 60270 - High-voltage test techniques - Partial discharge measurements (IEC 60270:2000) – 2001.
[2] F. Auzanneau, "Wire Troubleshooting and diagnosis: Review and perspectives", *Progress in Electromagnetics Research B*, Vol. 49, 2013
[3] S. Refaat, M. Sham – "A Review of Partial Discharge Detection, Diagnosis Techniques in High Voltage Power Cables" - IEEE Int. Conf. on Comp. Pow. Elect. and Power Eng., 2018.
[4] G. Fulli, F. Profumo, and E. Bompard, Electricity Security in the EU: Features and Prospects, Joint Res. Centre, Brussels, Belgium, Aug. 2018.
[5] C. C. Yii, M. N. K. H. Rohani, M. Isa, and S. I. S. Hassan, "Multi-end PD location algorithm using segmented correlation and trimmed mean data filtering techniques for MV underground cable," *IEEE Trans. on Dielectrics and Electrical Insulation*, vol. 24, no. 1, Feb. 2017.
[6] F. P. Mohamed, W. H. Siew, J. J. Soraghan, S. M. Strachan, "Partial Discharge Location in Power Cables using a Double Ended Method Based on Time Triggering with GPS", IEEE *Transactions on Dielectrics and Electrical Insulation*, Vol. 20, No. 6; Dec 2013.
[7] M. S. Mashikian, R. Bansal, R. B. Northrop – "Location and Characterization of Partial Discharge sites in Shielded Power cables", *IEEE Trans. on Pow. Del*., Vol. 5, No.2, April 1990.
[8] G. Robles, M. Shafiq, J. M. Martínez-Tarifa, "Multiple Partial Discharge Source Localization in Power Cables Through Power Spectral Separation and Time-Domain Reflectometry", *IEEE Trans. on Instrumentation and Measurement*, Vol. 68, No. 12, Dec. 2019.
[9] G. Zhu; K. Zhou; S. Zhao; Y. Li; L. Lu, "A Novel Oscillation Wave Test System for Partial Discharge Detection in XLPE Cable Lines", *IEEE Trans. Power Del*, Vol. 35, no. 4, pp. 1678-1684 Aug. 2020.
[10] J. Zhon, X.Bi, Q. Shu, , M. Chen, D. Zhou, D. Zhang, "Partial Discharge Signal Denoising Based on Singular Value Decomposition and Empirical Wavelet Transform" *IEEE Trans. on Instrumentation and Measurement*, Vol. 69, No. 11, Nov. 2020.
[11] S. Zhou, J. Tang, C. Pan, Y. Luo, K. Yan, "Partial Discharge Signal Denoising Based on Wavelet Pair and Block Thresholding", IEEE Access, June 30, 2020.
[12] F. Rachidi, M. Rubinstein, M. Paolone, *Electromagnetic Time Reversal – Application to Electromagnetic Compatibility and Power System* - John Wiley & Sons Ltd, 2017; pp. 95-97.
[13] A. Ragusa, H. Sasse, A. Duffy, F. Rachidi, M. Rubinstein, "Electromagnetic Time Reversal Method to Locate Partial Discharges in Power Networks using 1D TLM modelling", *IEEE Letters on EMC Practice and Applications*, Vol.3, No 1, March 2021.
[14] A. Ragusa, H. Sasse, A. Duffy, F. Rachidi, M. Rubinstein – "Application to Real Power Networks of a Method to Locate Partial Discharges Based on Electromagnetic Time Reversal", accepted by *IEEE Trans. on Power Delivery* in July 2021.
[15] A. Ragusa, H. Sasse, A. Duffy, "On-Line Partial Discharge Localization in Power Cables Based on Electromagnetic Time Reversal Theory - Numerical Validation", accepted by *IEEE Trans. on Power Delivery* in July. 2021.
[16] A. Ragusa, H. Sasse, A. Duffy, "Electromagnetic Time Reversal to Locate Partial Discharges in Power Networks with Inhomogeneous cables using the Transmission Line Matrix Method"- *CIGRE Science and Engineering Journal*, June 2021.
[17] H. Karami, M. Azadifar, A. Mostajabi, M. Rubinstein, F. Rachidi, "Numerical and Experimental Validation of Electromagnetic Time Reversal for Geolocation of Lightning Strikes" *IEEE Tran. on EMC*, Vol. 62, No. 5, Oct. 2020.
[18] S.Y. He, Y.Z. Xie, Z. Wang, F. Rachidi, B.Y. Liu, Q Li, X. Kong - "Norm Criteria in the Electromagnetic Time Reversal Technique for Fault Location in Transmission Lines ", *IEEE Trans. on EMC*, Vol. 60, No. 5, pp. 1240 - 1248, Oct. 2018.
[19] P. Wagenaars, P. A. A. F. Wouters, P. C. J. M. van der Wielen, E. F. Steennis, "Influence of ring main units and substations on online partial-discharge detection and location in medium-voltage networks," *IEEE Trans. Power Delivery*, vol. 26, no. 2, pp. 1064-1071, Apr. 2011.
[20] P. Wagenaars, "Integration of online partial discharge monitoring and defect location in medium-voltage cable networks," Ph.D. dissertation, Dept. Electr. Eng., Eindhoven University of Technology, 2010.
[21] C. Christopoulos, The transmission-line modeling method – TLM, Wiley-IEEE Press, 1995
[22] Integrated Engineering Software, Electro and Oersted versions 11.0. https://www.integratedsoft.com; last accessed 22-08-2021.

Antonella Ragusa, (M'08) received the Master and Ph.D. degrees in Electrical Engineering from the University of Palermo, Italy, in 2001 and 2006, respectively. In 2007, she worked at FIAT. She has been a permanent researcher at the Institute of Marine Engineering (INM) of National Research Council (CNR) of Italy, Palermo since 2008. Currently, she is a Marie Curie Researcher Fellow (MSCA-IF) at De Montfort University of Leicester, UK. Her research interests include electromagnetic compatibility, computational electromagnetics and smart grids.

Peter A. A. F. Wouters studied physics at Utrecht University (UU), Utrecht, the Netherlands, until 1984, from where he received the Ph.D. degree for a study on elementary electronic transitions between metal surfaces and low energetic (multiple) charged ions in 1989. In 1990, he joined the Electrical Energy Systems (EES) Group, Eindhoven University of Technology, as a Research Associate. Since 2003, he has been an Assistant Professor in the field of diagnostic techniques in HV systems. From 2018 until 2021, he was appointed as a Visiting Professor with the College of Chemical and Biological Engineering, Zhejiang University in Hangzhou, China. His research interests include partial discharge techniques, vacuum insulation, and LF electromagnetic field shielding.

Hugh G. Sasse, received the B.Sc. (Hons) degree in electronic engineering from the University of York, York, U.K., in 1985, and has received his PhD. degree in 2010 from De Montfort University, Leicester, U.K. His research is on optimization of physical layer components for communications systems at De Montfort University.

Alistair Duffy, (SM'04, F'14), is Professor of Electromagnetics and Director of the Institute of Engineering Sciences at De Montfort University (DMU), Leicester, UK. He received his BEng (Hons) and MEng degrees in 1988 and 1989, respectively, from University College, Cardiff, University of Wales. He read for his PhD with professors Christopoulos and Benson at Nottingham University, graduating in 1993. He also holds an MBA from the Open University, UK, graduating in 2004. He was awarded his DSc from Cardiff University in 2019 for his body of research on the validation of computational electromagnetics. He is a Fellow of the IEEE and President of the IEEE EMC Society. He has published approximately 300 papers, mostly on his research interests of validation of computational electromagnetics; physical layer components, particularly communications cabling, and electromagnetic compatibility testing.